NJC

Accepted Manuscript

This is an *Accepted Manuscript*, which has been through the Royal Society of Chemistry peer review process and has been accepted for publication.

Accepted Manuscripts are published online shortly after acceptance, before technical editing, formatting and proof reading. Using this free service, authors can make their results available to the community, in citable form, before we publish the edited article. We will replace this *Accepted Manuscript* with the edited and formatted *Advance Article* as soon as it is available.

You can find more information about *Accepted Manuscripts* in the Information for Authors.

Please note that technical editing may introduce minor changes to the text and/or graphics, which may alter content. The journal's standard Terms & Conditions and the Ethical guidelines still apply. In no event shall the Royal Society of Chemistry be held responsible for any errors or omissions in this *Accepted Manuscript* or any consequences arising from the use of any information it contains.

ROYAL SOCIETY OF CHEMISTRY

www.rsc.org/njc

Design and synthesis of novel trinuclear palladium (II) complex containing oxime chelate ligand; Determining interaction mechanism with DNA groove and BSA site I by spectroscopic and molecular dynamics simulation approaches

Kazem karami[a], Zohreh Mehri Lighvan[a], Somayeh Asgari barzani[a], Ali Yeganeh Faal[b], Marziyeh Poshteh-Shirani[a], Taghi Khayamian[a],Václav Eigner[C], Michal Dušek[C]

[a]*Department of Chemistry, IsfahanUniversity of Technology, Isfahan, 84156/83111, Iran*
[b]*Department of Chemistry, Faculty of Science, Payam Noor University, Iran*
[c]*Institute of Physics AS CR, v.v.i.,Na Slovance 2, Prague 8, Czech Republic*

ABSTRACT

The novel trinuclear Pd (II) complex with aryl oxime ligand, $[Pd_3(C,N\text{-}(C_6H_4C(Cl)=NO)\text{-}4)_6]$ was synthesized and structurally characterized by elemental analysis (C, H, N), IR, resonance signals in the NMR, and single crystal X-ray crystallography. The interaction ability of the complex with native calf thymus DNA (CT-DNA) was monitored as a function of the metal complex-DNA molar ratio by UV-Vis absorption spectrophotometry, fluorescence spectroscopy, circular dichroism (CD) and thermal denaturation methods. All the experimental evidence indicated this complex could strongly bind to CT-DNA via a groove mechanism. Further, the albumin interactions of complex were investigated using fluorescence quenching and synchronous fluorescence spectra. The result of fluorescence titration suggested that the fluorescence quenching of BSA by complex was a static quenching procedure. The site marker displacement experiment has suggested the location of complex binding to BSA was Sudlow's site I in the subdomain IIA. Finally, the molecular docking experiment confirmed the above results and effectively proved the binding of Pd (II) complex to BSA and DNA.

Keyword: Pd complex; Oxime; CT-DNA binding; BSA binding; Crystal structure

---

[1]Correspondingauthor: KazemKarami; *Tel: +983133913239; fax: +983133912350*

E-mail addresses:karami@cc.iut.ac.ir(K. Karami), z.mehri@ch.iut.ac.ir(Z. MehriLighvan).

Introduction

Nowadays, tumor resistance to drug is one of the most important problems in the cancer treatment [1,2]. Cisplatin, one of the most potent chemotherapy drugs, widely used for cancer treatment. Despite its broad clinical applications, the resistance of cancer cells to cisplatin often culminates in chemotherapeutic failure [3-6]. On the other hand, the discovery of cytotoxic properties of cisplatin provided enormous impetus for research into the use of transition metal complexes in fighting against cancer. Where platinum drugs are ineffective, the mortality from cancer is significantly higher than when they are effective. As a result, new transition metal-based compounds are being designed to overcome the platinum complex limitations. Owing to the similar coordination modes of the cation Pd (II) and Pt (II) (d^8-electron configuration) there has also been renewed interest in attempt to obtain activity for palladium (II) complexes [7-11]. Palladium (II) analogues of platinum (II) complexes are about 10^4-10^5 time more reactive. To minimize the high lability and fast hydrolysis of palladium complexes in biological environments, chelating ligands were used to synthesize the antitumor agents [12]. Furthermore, new mononuclear, dinuclear, and multinuclear palladium complexes with decreased toxicity have been developed, which are also effective in cisplatin-resistant tumors [13,14]. Among Pd (II) complexes, special attention has been paid to those with such nitrogen donor ligands as derivatives of ethylenediamine, diaminocyclohexane, ammonia, pyridine, quinoline, pyrazole, and oxime, which have shown promising antitumor characteristics in vivo and in vitro [15-16]. Oxime derivatives have attracted wide interest because of their antibacterial, antifungal properties [17], and a high index of antitumor activity [18,19] via intercalation. In addition, the biological relevance of oximes appreciably favors their use as ligands for potential metal-based drugs. For instance, it was reported that oxime complexes and other species bearing the oxime

functional group caused biological effects such as endothelium-independent relaxation in blood vessels,[20,21] an increase in the targeting of specific nuclear bases of DNA[22], and oxidative DNA cleavage as well [23]. Since DNA is an important cellular receptor, many chemicals exert their antitumor effects to DNA there by changing the replication of DNA and inhibiting the growth of tumor cell. Additionally, studies on the interaction of transition metal complexes with DNA have been pursued in recent years [24]. In general, most components have three distinct modes of non-covalent interaction with DNA, i.e. intercalative association, DNA groove binding and electrostatic attraction [25]. On the other hand, one of the important properties of a drug is the degree of its protein binding which affects the drug effective solubility, bio distribution, and its half life in the body. Proteins are the most abundant macromolecules in cells and are crucial to maintaining normal cell functions. Among bio macromolecules, the serum albumins which have many physiological functions are the major soluble protein constituent of the circulatory system [26]. Interaction of transition metal complexes to albumins may provide useful structural information that determines the therapeutic effect of drugs. Therefore, the investigation on the binding of such molecules with BSA is of imperative and great importance in life sciences, chemistry, and clinical medicine [27,28]. In previous studies we exhibited that NC palladacyclic and Pt complexes have reasonable cytotoxic effects against some tumor cell lines and good DNA/BSA binding affinity [29-31]. In the present study we aimed to investigate anticancer properties of a new Pd (II) complex containing chelating oxime ligand and understand the structure–activity relationships (SARs) of this new chemical compound. The studies on the DNA and protein binding interaction of palladium complexes containing the oxime N,O chelating have not yet been reported. In this paper, we studied the new complex from the four aspects: (i) synthesis and characterization of the complex by means of spectroscopic and X-ray diffraction

studies; (ii) study of the ability of the complex to interact with DNA and investigation of its interaction mechanism using UV-Vis and fluorescence spectroscopy, thermal denaturation, and circular dichroism (CD) spectra ; (iii) monitoring of the protein binding ability by UV absorption and tryptophan fluorescence quenching experiment in the presence of the complex using BSA as a model protein; (iv) the molecular dynamics (MD) simulations performed on the structure of BSA and DNA.

Experimental Section

Materials

Starting materials and solvents were purchased from Sigma-Aldrich or Alfa Aesar and used without further purification. Calf thymus DNA (CT-DNA) and BSA was obtained from Sigma-Aldrich and were used as supplied. 4-chlorobenzoxime was obtained using the procedure described [32]. The DNA concentration per nucleotide was determined by absorption spectroscopy using the molar absorption coefficient (ε =6600 M^{-1} cm^{-1} at 260 nm) [33]. The stock solutions were stored at 5 °C and used over no more than 4 days. All the experiments involving interactions of the compounds with DNA were carried out in double distilled water buffer containing 5 mM Tris-HCl [tris (hydroxymethyl)-aminomethane] and 50 mM NaCl, and adjusted to pH 7.4 using NaOH. A stock solution of the Pd (II) complex was prepared by dissolving the complex in an aqueous solution of DMSO as the co-solvent, and then diluted suitably with the corresponding buffer to the required concentrations for all the experiments. The final DMSO concentration never exceeded 0.5% v/v.

Physical measurements

The UV–Vis spectra were recorded on a Varian Cary 100 UV–Vis spectrophotometer using a 1 cm path length cell. Infrared spectra were recorded on a FT-IR JASCO 680 spectrophotometer in the spectral range 4000-400 cm^{-1} using the KBr pellets technique. NMR spectra were measured

on a Bruker spectrometer at 400.13 MHz (^{1}H), 100.61 MHz ^{13}C–{^{1}H}, Elemental analysis was performed on a Leco, CHNS-932 apparatus. The T_m spectra were recorded on a Varian BioCary-100 UV-Vis spectrophotometer using a 1 cm path length cell. Circular dichroism measurements were carried out on a Jasco-810 spectropolarimeter at room temperature with a rectangular quartz cell of 1 cm path. Solution was prepared by dissolving the complex in water buffer containing 5 mM Tris–HCl (pH 7.4) and 50 mM NaCl concentrations.

Synthesis of Pd (II) complex

Preparation of $[Pd_3(C,N\text{-}(C_6H_4C(Cl)=NO)\text{-}4)_6]$: 4-Chlorobenzoxime (309 mg, 2mmol) and pyridine (0.17 ml, 2 mmol) were added to a solution of palladium acetate (224 mg, 1 mmol) in $CHCl_3$ (15 ml). The resulting orange–red solution was refluxed for 4 h (Scheme 1). Following addition of water (10 ml), the product was extracted with chloroform (3 × 15 ml) and then filtered through a plug of MgSO4. The filtrate was concentrated to ca. 2 mL and to this concentrated solution, n-hexane (15 mL) was added to precipitate a yellow solid, which was collected and air-dried. bright yellow crystals of complex were obtained from $CHCl_3$,n-hexane. Yield: 85%. Anal. Calc. for $C_{42}H_{30}Cl_6N_6O_6Pd_3$: C 40.3; H 2.7; N 6.7%. Found. C 42.99; H 2.35; N 6.7%. IR (KBr pellet, cm^{-1}): ν (C=N) = 1626, ν (OH) = 3303, ν (N-O) = 1012, ν (C-$H_{aromtic}$)= 3067. ^{1}H NMR (400.13 MHz, $CDCl_3$, ppm): δ=7.24(s,1H,C_6H_4Cl), 7.26(s,1H,C_6H_4Cl),7.851-7.854 (d,2H,C_6H_4Cl), 7.87(s,1H,CH).^{13}C–{1H} NMR (100.61 MHz, $CDCl_3$, ppm): 124.6 (s,C_2),128.6(s, C_3,C_7),129 (s, C_4,C_6),136.3(s, C_5),150.5(s, C_1).

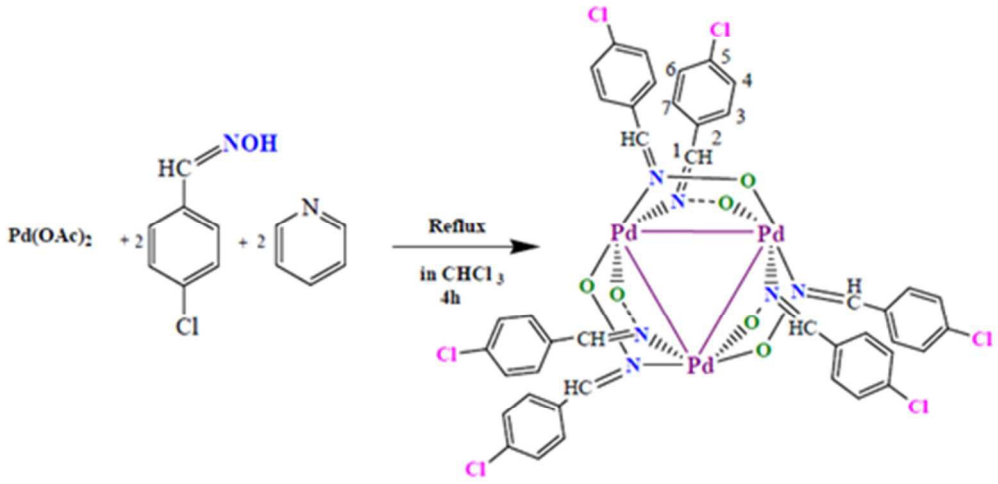

Scheme 1. Synthesis of the trinuclear palladium complex.

Single-crystal structure determination

X-ray diffraction experiment was done at 120 K with the use of Agilent Gemini single crystal diffractometer (Cu Kα radiation). The structure was solved using Super flip software [34] and further refined with Jana2006 [35]. MCE software [36] was used for Fourier maps visualization. The structure was refined by full matrix least squares on F squared value. The atoms of palladium complex were refined anisotropically, the positions of hydrogen atoms were kept in expected geometry with U_{iso} set to 1.2 of U_{eq} of the parent atom. The atoms O_1, O_2 and O_3 were refined isotropically and they represented disordered solvent. The centers of these atoms do not represent actual atomic positions. For further details on data collection and structure refinement see table 1.

Molecular docking . The molecular docking was performed by Autodock 4.2 package using the Lamarckian genetic algorithm (LGA) method [37]. Molegro Virtual Docker (MVD) [38] and UCSF Chimera [39] packages were used to produce molecular images and animations. The

schematic two-dimensional representations of the docking results were performed using LIGPLOT+ [40].

Molecular dynamics (MD) simulations on BSA and DNA. The molecular dynamics (MD) simulation was performed on the structure of BSA and DNA in a water box. The crystal structure of BSA was obtained from the protein data bank (PDB ID: 4F5S) at a resolution of 2.47 Å. Also, the DNA sequence d(CGCGAATTCGCG)$_2$ was taken from the protein data bank (PDB ID: 1BNA) at a resolution of 1.90 Å. The MD simulations were carried out using the GROMACS 4.5.1 package [41]. The topology parameters of BSA and DNA were created by the GROMOS96 43a1 [41] and Amber99 force field [42], respectively. The interaction parameters were computed using intermolecular (non-bonded) potential represented as a sum of Lennard–Jones (LJ) force and pairwise Coulomb interaction and the long-range electrostatic force determined by the Particle-Mesh Ewald (PME) method [43,44]. The velocity Verlet algorithm was used for the numerical integrations [45], and the initial atomic velocities were generated with a Maxwellian distribution at the given absolute temperature [46,47]. The BSA and DNA systems were subjected to a cubic box ($8.17 \times 8.17 \times 8.17$ nm^3) and ($7.54 \times 7.54 \times 7.54$ nm^3), respectively. The water molecules were added using a simple charge (SPC216) model [48] and the solvated systems were neutralized by adding sixteen and twenty-two Na^+ ions in the simulation, respectively. Initially, the energy minimization was performed before implementing the position restraint procedure. Then, the full system was subjected to 6000 ps MD at constant pressure (1 bar) and constant temperature (310 K) using the Berendsen thermostat [49].

The MD simulations were carried out on the open SUSE 11.3 Linux on an Intel Core 2 Quad Q6600 2.4 GHz and 4 GB of RAM. The stability of two systems and the structural geometries were tested by means of the root-mean-square deviations (RMSDs).The root-mean square

deviations (RMSDs) between the backbone atoms of the trajectory frames of BSA and DNA with the corresponding atoms of the X-ray structure was calculated for each ps of MD simulation. The average RMSDs value of BSA and DNA backbone was calculated to be 8.33and 5.21 nm, respectively. The equilibrated conformation of the BSA and DNA were used for docking.

Results and discussion

Synthesis and spectroscopic characterization

The palladium aryl oxime complex $[Pd_3(C,N\text{-}(C_6H_4C(Cl)=NO)\text{-}4)_6]$ is obtained in one step by reaction of $[Pd(OAc)_2]$ with 4-Chlorobenzoxime and pyridine in $CHCl_3$ under reflux for 4 h (Scheme1). This yellow Compound, stable at room temperature, is soluble in such chlorinated solvents as CH_2Cl_2, $CHCl_3$, and aprotic solvent like DMSO (dimethylsulfoxide). The compound was characterized by bands in the IR spectra, elemental analysis (C, H, N), resonance signals in the NMR, and single crystal X-ray crystallography.

The IR spectra of the complex showed typical bands at 3303,3067 and 1012 cm^{-1}assigned to ν (OH), ν (C-H aromtic) and ν (N-O), respectively. The oxime complex shift in ν (N-O) of the free ligand (960 cm^{-1} region) to higher wave number, ν (C=N) stretch at 1626 cm^{-1} was shifted to lower wave numbers (as compared to the free ligand) due to N-coordination of the oxime [50]. The NMR spectrum of complex was in good agreement with the proposed structure. In the ^1H NMR spectra (see Scheme 1 for labeling) exhibit signals in the range 7.24 (ppm) and 7.26 (ppm) due to the H_3 and H_7 protons of the oxime ligand. The aromatic protons are diastereotopic resulting in formation of two separated signals (Fig1). Moreover, the ^1H NMR spectra somewhat similar patterns for the H_4−H_6 aromatic protons of oximering, Where as H_1 is significantly shifted to high frequencies in the range 7.87 (ppm) due to the anisotropic deshielded from the

oxime ring or C=N group. The $^{13}C\{^{1}H\}$ NMR spectrum reveals the resonance for the CNO carbon atom of the oxime group at δ =150.3 ppm. As expected, four resonances are observed of the trinuclear complex, ipso-carbon atom (C2 δ =124.6 ppm), (C3,C7δ =128.6 ppm), (C4,C6 δ =129 ppm), (C5 δ =136.3 ppm) of the heterocyclic ligands.

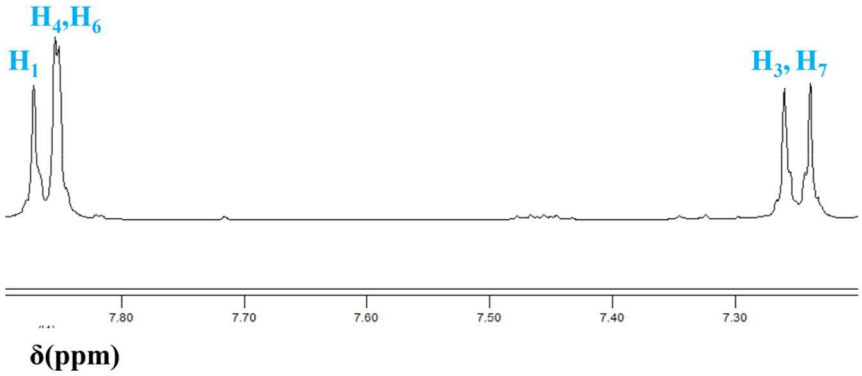

Fig. 1. The protons of the trinuclear palladium complex in the 1HNMR spectra.

Molecular structure of the complex

The investigated complex was characterized in the solid phase by a single crystal X-ray diffraction study. Yellow single crystals were obtained at room temperature by slow diffusion of n-hexane into dichloromethane or chloroform solution of the complex. Molecule of the compound is displayed in (Fig.2) with ADP ellipsoids at 50% probability level. Relevant crystallographic data and structure refinement details are listed in Table 1. Selected bond lengths and angles are listed in Table 2.The palladium oxime complex forms trimeric units featuring three six-membered rings (Pd–N–O–Pd–O–N) which consist of alternating palladium and oxime functional groups. C–H···π interactions play major role in complex packing, since no classical hydrogen bonds are present in the structure. The stacking of complex molecules creates cavities

in the structure which occupied by heavily disordered solvent molecules. The tri-nuclear complex is held by Pd–N, Pd–O, N–O as well as Pd–Pd bonds. The Pd–N bond lengths are 2.008(11) and 2.026 (12) Å, Pd–O bond lengths are 2.023 (10) and 2.027 (10) Å, N–O bond lengths are 1.338(1) and 1.341 (1) Å and Pd–Pd bond length is 2.894 (2) Å. The values are comparable to those observed in related complexes such as $[Pd_3(ON{=}CPr^{i}Ph)_6]$ (av.Pd– N = 2.016 Å, Pd–O =2.025 Å, N–O =1.339 Å), which also features bridging oxime groups [51].

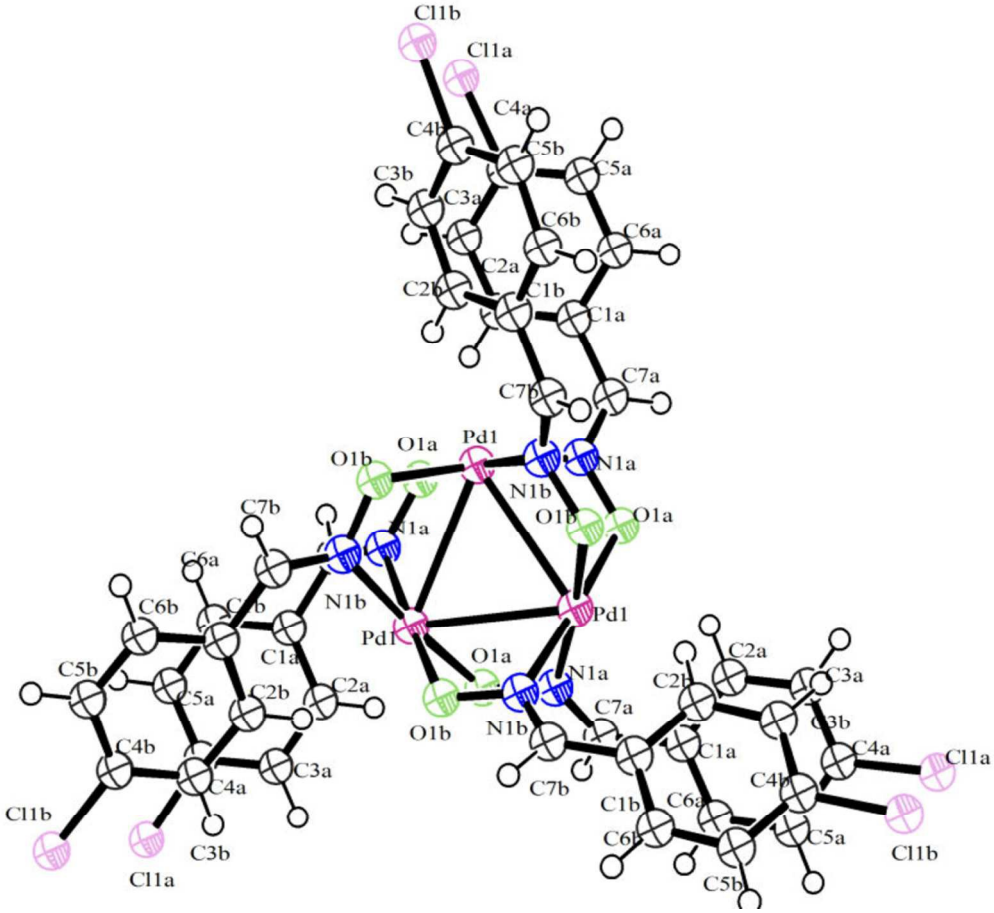

Fig. 2. ORTEP diagram for Pd complex with ellipsoids drawn at the 50%probability level.

Table 1. Crystallographic data and structure refinement details for Pd complex

Compund	Complex
Empirical formula	$C_{42}H_{30}Cl_6N_6O_6Pd_3 \cdot 5(O)$
Formula weight	1326.7
Crystal system	Trigonal
Space group	R-3
a / Å	18.766 (3)
c / Å	24.688 (2)
V / Å^3	7529.4 (15)
T / K	120
Z	6
ρ_{calc} / g cm^{-3}	1.756
μ / mm^{-1}	12.05
Crystal dimensions / mm	0.13 x 0.11 x 0.05
Reflections collected	15119
Independent reflections (Rint)	2963 (0.098)
GOF	1.37
R1, wR2 [I>3σ(I)]	0.073, 0.165
R1, wR2 (all data)	0.127, 0.196
Res. el. dens. (e Å^{-3})	1.31, -0.42
CCDC number	1058050

Table 2. Selected bond lengths (Å), and angles (°) for Pd complex.

Atoms	*Bond lengths*
Pd1—N1b	2.008(11)
Pd1—N1a	2.026(12)
Pd1—O1b	2.027(10)
Pd1—O1a	2.023(10)
Pd1—Pd1^{i}	2.894(2)
O1a—N1a^{ii}	1.338(18)
O1b—N1b^{ii}	1.342(17)
	Bond angles
N1a—Pd1—O1b	174.3(4)
N1b—Pd1—O1a	175.8(4)
N1b—Pd1—O1b	90.7(4)
O1a—Pd1—N1a	93.1(4)
O1a—Pd1—O1b	91.3(4)
N1b—Pd1—N1a	84.8(4)

Symmetry code: (i)-y, x-y, z (ii) –x+y, -x, z

DNA-binding mode and affinity

Electronic absorption titration. Monitoring the changes in absorption spectra of the test transition metal complexes upon the incremental addition of DNA is one of the most widely used methods to determine overall binding constants. Thus, in order to provide evidence for the possibility of binding of each complex to CT-DNA, spectroscopic titration of a solution of the Pd complex with CT-DNA was performed [52].DNA provides three distinct binding sites for transition metal complexes (groove binding, electrostatic binding to phosphate group and intercalation) [53–55].In general, hypochromismand hyperchromism are known to cause

spectral changes typical of metal complexes associated with DNA helices. The binding of an intercalative molecule to DNA is accompanied by hypochromism and a significant red-shift (bathochromism) is characteristic of strong π–π stacking interaction between the aromatic chromophore of the ligand of a metal complexes and DNA base pairs [56]. On the other hand, groove binding results only in a small shift in the absorption spectra [57,58]. As shown in (Fig.3), the potential CT-DNA binding ability of complex was studied by UV spectroscopy by following the intensity changes of the intraligand π-π* transition band at 252, 305 nm. In details, the absorption band (λ_{max}=252) in the presence of increasing concentrations of CT-DNA, a significant hypochromic (H% = 14.21) and only in a small shift in wavelength. the observation is ascribed to groove binding [59].

In order to further investigate the intensity of the interaction between the complex and CT-DNA, the intrinsic binding constant, K_b were calculated according to equation (1)[60].

$$\frac{[DNA]}{(\varepsilon_a-\varepsilon_f)} = \frac{[DNA]}{(\varepsilon_b-\varepsilon_f)} + \frac{1}{K_b\,(\varepsilon_b-\varepsilon_f)} \quad (1)$$

The absorption coefficients ε_a, ε_f, and ε_b correspond to A_{obs}/[DNA], the extinction coefficient for the free complex and the extinction coefficient for the complex in the fully bound form, respectively. In particular, ε_f was determined by a calibration curve of the isolated Pd (II) complex in an aqueous solution, following Beer's law. The slope and the intercept of the linear fit of the plot of [DNA]/[ε_a-ε_f] versus [DNA] give 1/[ε_a-ε_f] and 1/Kb[ε_b-ε_f](Fig. 3, inset). The intrinsic binding constant K_b($1.5\times10^5 M^{-1}$)can be obtained from the ratio of the slope to the intercept [60].

From the values of the binding constant (K_b), free energy (ΔG) of the compound–DNA complex was calculated using the equation (2):

$$\Delta G = - RT \ln K_b \quad (2)$$

Binding constants are measure of the compound–DNA complex stability while the free energy indicates the spontaneity/non-spontaneity of compound–DNA binding. Free energy of Pd complex was evaluated as negative values (−6.58 kJ.mol^{-1}) showing the spontaneity of compound–DNA interaction.

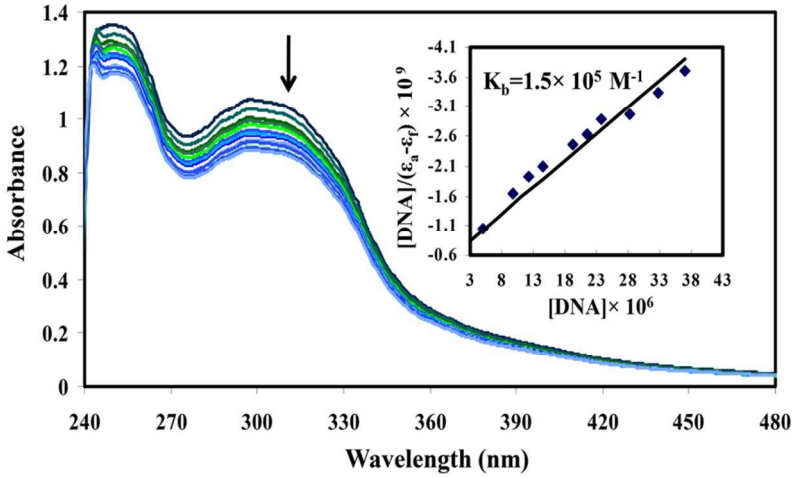

Fig. 3. Electronic spectra of complex in buffer solution (5 mM Tris–HCl/50 mM NaCl at pH 7.4) upon addition of CT-DNA. *C*(comlex) = 2.5×10^{-5}mol L^{-1} , *C*(DNA) = 0- 3.7×10^{-5}mol L^{-1}. Arrow shows the absorption intensities decrease upon increasing DNA concentration. Inset: Plots of [DNA]/[ε_a - ε_f] vs. [DNA] for the titration of complex with DNA.

Fluorescence studies Competitive interaction of complex with MB-ds-DNA. To check whether the binding of Pd (II) complex with DNA is of the groove or the intercalative nature, we performed a comparative binding study with Methylene blue. Methylene blue (MB), a phenothiazinium dye is known to bind with nucleic acids. The planar heterocyclic dye is expected to stabilize its binding to DNA through favorable stacking interactions with its adjacent base pairs [61]. The enormous quenching in the emission intensity of the MB in DNA

environment can be rationalized by considering the intercalative binding of MB with the DNA [62], and it is expected because of its strong stacking interaction (intercalation) between the adjacent DNA base pairs [63,64]. We have monitored the emission spectra of DNA bound MB in the presence of varying concentrations of the complex (Fig.4). The experiment revealed that addition of the complex to the DNA bound MB does not cause releasing MB molecules, while the emission intensity decreases steadily. This implies that the two probes, the complex and the MB, bind with DNA independently and binding of one probe does not affect the binding of the other. Fig. 4 clearly reveals the decrease in the fluorescence intensity of the probe molecule (MB) ([DNA]/[MB]=10) by adding the Pd(II) complex([complex]/[DNA]=2.5). Thus, the experiments confirmed that interaction between DNA and Pd (II) complex is the groove interaction.

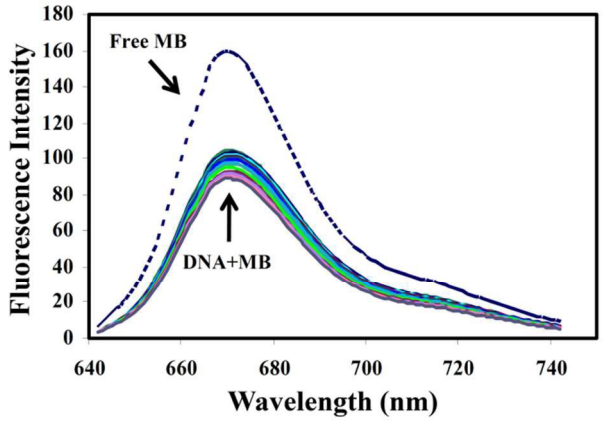

Fig. 4. The emission spectra of the DNA–MB system, in the presence of complex,*C*(DNA) = 5×10^{-5}mol L^{-1} , *C*(comlex) = 0–1×10^{-5}mol L^{-1} , *C*(MB) = 5×10^{-6}mol L^{-1} . The arrow shows the emission intensity changes upon increasing complex concentration.

Circular dichroism spectra. Circular dichroism spectra of DNA-type substances give information on the diagnosing changes in DNA morphology by their interaction with transition metal complexes as well as destabilization of the DNA helix [65].CT- DNA is the B-form DNA, CD spectrum of B form DNA consists of a positive band at 275 nm due to base-stacking and a negative band at 245 nm due to helicity [66]. The secondary structure of DNA is known to be perturbed by the intercalation of small molecules and thus increases intensities of the both bands stabilizing the right-handed B conformation of CT-DNA, whereas simple groove binding and electrostatic interaction show less or no perturbation on the base stacking and helicity bands. The CD spectra of DNA were monitored in the presence of the complex as shown in (Fig. 5).Gradual addition of the complex to DNA causes decrease of the CD spectra intensity in the positive band as well as in the negative band. Thus, the experiments confirm that the DNA binding of the complex induces certain conformational changes, such as the conversion from a more B-like to a more Z-like structure within the DNA molecule [67]. These changes are indicative of the groove binding mode [68,69].

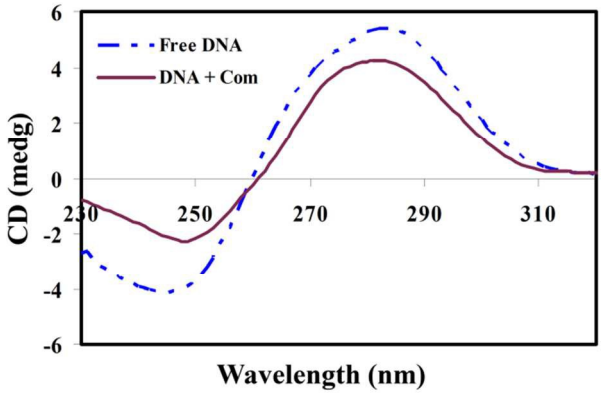

Fig. 5. CD of CT-DNA (1×10^{-4}mol L^{-1}) in the absence and the presence of Pd (II) complex (5×10^{-5}mol L^{-1}) in 5 mM Tris–HCl with 50 Mm NaCl (pH=7.4)

Melting of DNA helix on interaction with the Pd complex. Denaturation of double-stranded DNA (ds-DNA) is a very important phenomenon involving biological, chemical and physical consequences [70,71]. Upon increasing the temperature, hydrogen bonds between the double-helical structure of DNA base pairs start to cleave resulting in arandom coil. The melting temperature (T_m) is strongly related to the stability of the double-helical structure. So the transition temperature of double strands to single strands can be determined by monitoring the absorbance of the DNA bases at 260 nm as a function of temperature [72]. Generally, a ΔT_m of a few degrees Celsius is considered to be evidence of an interaction involving groove binding and/or electrostatic binding to the phosphate groups [73, 74], while an increase of over 10°C is attributed to an intercalation binding mode, due to the stabilization of the DNA double helix [75]. The melting curves of CT-DNA in the absence and presence of the complex are presented in (Fig 5). Here, T_m of CT-DNA was found to be 81.62◦C in buffer while after addition of the Pd (II) complex, the T_m of the DNA increased to 84.23◦C. This increase corresponds to that observed for groove binding [59].

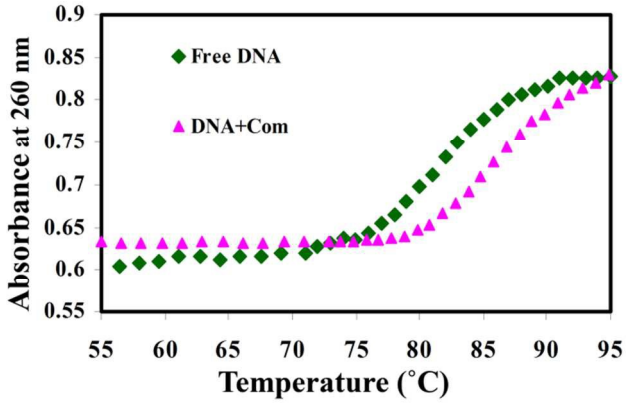

Fig. 6. Plots of the changes of absorbance at 260 nm of CT-DNA (7.5×10^{-6}mol L^{-1}) on heating in the absence and the presence of the complex (37.5×10^{-6}mol L^{-1}) in 5 mM Tris–HCl with 50 Mm NaCl.

Protein binding experiments

UV absorption spectra of BSA in the presence of the complex. UV–Vis absorption spectra experiment is performed to identify the real mechanism of this quenching procedure [76]. (Fig.7) shows the UV absorption spectra of BSA in the presence of different concentrations of the complex. The absorbance spectrum of BSA shows two characteristic bands. One is located in the range of 220–240 nm, which is the skeleton absorption peak (α-helix structure), and the other is at 278 nm, which is the absorption band of the aromatic amino acids (Trp, Tyr, and Phe). (Fig.7) indicates that upon adding the complex, the BSA skeleton absorption intensity in the range of 220–240 nm decreases and red shifts appear due to the perturbation of the secondary structure of the protein [77-78] and subtle change the maximum absorption at 278 nm, which indicated a perturbation of α-helix induced by a specific interaction between Pd complex and BSA [79-80].

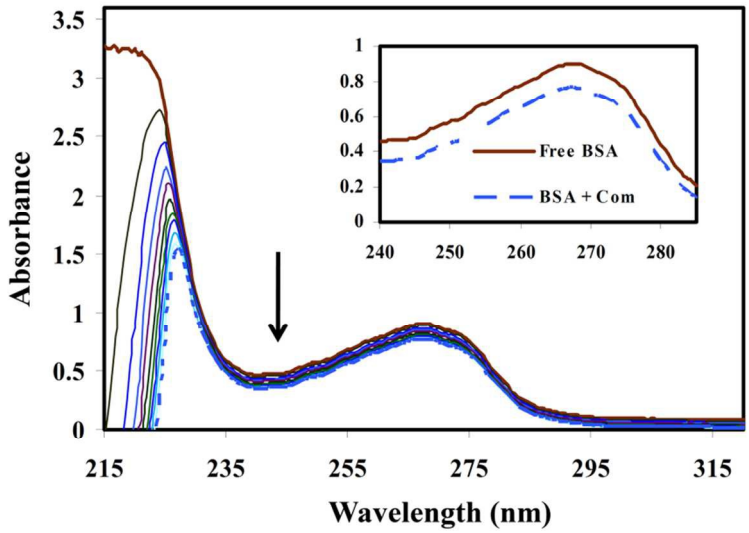

Fig. 7. UV absorption spectra of *C*(BSA) =2×10^{-6}mol L^{-1}in the absence and presence of complex.*C*(comlex) =0,5.94×10^{-7} ,1.17×10^{-6},1.74×10^{-6},2.30×10^{-6},2.85×10^{-6},3.39×10^{-6},3.92×10^{-6}, 4.44×10^{-6} ,5.45×10^{-6},6.42×10^{-6}mol L^{-1} .in 5 mM Tris–HCl with 50 Mm NaCl.

Tryptophan quenching experiment. Fluorescence spectroscopy is an important method to probe the structure and dynamics of bio macromolecules. Fluorescence quenching refers to the decrease found in the fluorescence intensity due to the environmental alteration around the fluorophore, which can reveal the nature of binding reaction [81]. Generally, the fluorescence of protein is caused by three intrinsic characteristics of the protein, namely tryptophan, tyrosine, and phenyl alanine residues. Actually, the intrinsic fluorescence of many proteins is mainly contributed by tryptophan alone. The emission intensity depends on the degree of exposure of the two tryptophan side chains [82], 134 and 212, to polar solvent. It is evident from (Fig. 8) that fluorescence emission intensities of BSA at 345 nm show remarkable decreasing trend with increasing concentration of the complex. This suggests a change in the conformation of BSA [83].The fluorescence intensity data were then analysed according to Stern-Volmer relation equation (3) to get a better insight into the type of quenching:

$$F_0/F = 1 + K_{sv}[Q] = 1 + K_q\tau_0[Q] \quad (3)$$

where F and F_0 are the fluorescence intensity of BSA with and without quencher (complex), respectively. Kq, K_{SV}, τ_0 and [Q] are the quenching rate constant of the biomolecule, the dynamic quenching constant, the average lifetime of the biomolecule without quencher and the concentration of quencher, respectively. Obviously, since the fluorescence life time of biopolymer is 10^{-8} s . In the present work, the value of Kq was observed to be 5.16×10^{13} $Lmol^{-1}$ s^{-1} at 298K can be calculated using the fallowing equation:

$K_q = K_{sv}/\tau_0$

However, the maximum scatter collision quenching constant, Kq of various quenchers with the biopolymer is 2×10^{10} $Lmol^{-1}$ s^{-1}[84]. Thus, the rate constant calculated by protein quenching

procedure is greater than Kq of the scatter procedure. This indicates that a static quenching mechanism is operative [85,86].

Therefore, the fluorescence quenching of BSA by complex should be analyzed using the modified Stern–Volmer equation equation (4). [87]:

$$\frac{F_0}{\Delta F} = \frac{1}{f_a K_a}\frac{1}{[Q]} + \frac{1}{f_a} \qquad (4)$$

where K_a is the association constant for the accessible fluorophores, f_a is the fraction of accessible fluorescence, ΔF is the difference in fluorescence intensity between the absence and presence of quencher at concentration [Q], The dependence of $F_0/\Delta F$ on the reciprocal value of the quencher concentration $[Q]^{-1}$ is linear, with slope equal to the value of $(f_a K_a)^{-1}$. A quantitative estimate of the extent of binding (K_a), is determined from the intercept to slope ratio of the modified Stern–Volmer equation. The K_a value for BSA–Com system is computed as 1.89×10^5 L mol^{-1}.

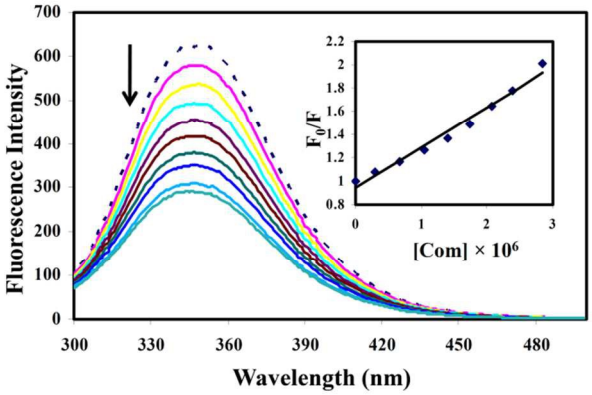

Fig. 8. Emission spectra of BSA upon the titration of complex.*C*(BSA) = 2×10^{-6} mol L^{-1}, *C*(comlex) =0,2.95×10^{-7} ,6.76×10^{-7},1.04×10^{-6},1.39×10^{-6},1.73×10^{-6},2.06×10^{-6},2.37×10^{-6},2.83×10^{-6} mol L^{-1}. Arrow shows the change upon the increasing complex concentration. Inset: Plots of F_0/F vs. (complex) for the titration of the complex to BSA.

Determination of binding number and binding site on BSA. When complexes bind independently to a set of equivalent sites on a macromolecule, the binding constant (K_{bin}) and the number of binding sites (n) can be obtained from fluorescence intensity data [88]:

$$\mathrm{Log}\frac{(F_0 - F)}{F} = \mathrm{Log}\, K_{bin} + n\, \mathrm{Log}\,[Q] \quad (5)$$

where F_0 and F have the same meaning as in equation (3), n is the average binding number for one complex and K_{bin} is the binding constant. The double logarithmic plot of log[F_0-F/F] vs. log[com] is shown in (Fig. 9). For the system complex and BSA, the obtained values of K_{bin} and n at 298K were 3.26×10^5 L mol^{-1} and 0.864, respectively. Moreover, the linear correlation coefficient was calculated to be 0.9914, which indicated that the assumptions underlying the derivation of equation (5) were satisfied. The value of n close to 1 indicated that there was single class of binding site for complex on BSA. The binding free energy for the complex to BSA was found to be –7.56kJ.mol^{-1}.

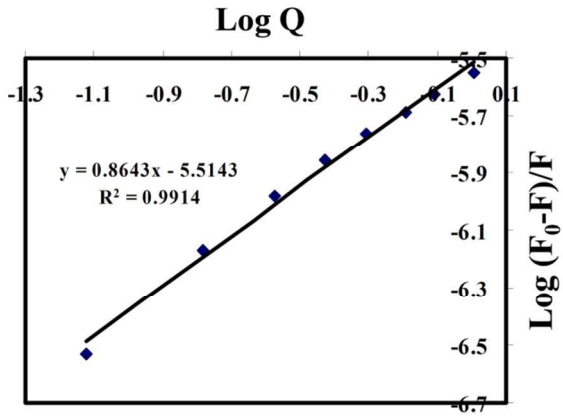

Fig. 9. Scatchard plots of log [(F_0−F)/F] vs log [Q] for determination of the complex-BSA binding constant and the number of binding sites on BSA for complex.

Site marker-competitive binding experiments. The drug competition for binding sites on serum albumin can also affect the free and bound forms of the complex. Therefore, it is important to identify the binding site of the complex in BSA. Crystal structure of BSA shows that BSA is a heart-shaped helical monomer composed of three homologous domains named I, II, III, and each domain includes two sub-domains A and B to form a cylinder. The principal regions of complex-binding sites on albumin are located in the hydrophobic cavities in sub-domains IIA and IIIA with similar chemical properties, called Sudlow's sites I and II, respectively [89,90]. In order to identify the complex-binding site on BSA, site marker competitive experiments are carried out, using markers which specifically bind to a known site or region on BSA. From X-ray crystallography studies, Eosin Y has been demonstrated to bind to the sub-domain IIA while ibuprofen is considered as sub-domain IIIA binder [91-92]. Information about the complex-binding site can be gained by monitoring the changes in the fluorescence of the complex bound albumin that brought about by site I (Eosin Y) and site II (ibuprofen) markers. Then information on the binding site that complex binds to can be obtained by monitoring the changes of the fluorescence of BSA after binding complex, in the presence of Eosin Y and ibuprofen. As shown in (Fig. 10A and B), with the addition of site marker (Eosin Y or ibuprofen) into BSA, the fluorescence intensity is lower than that of without site marker. To facilitate the comparison of the influence of Eosin Y and ibuprofen on the binding of complex to BSA, the binding constant in the presence of site markers was analyzed using the equation (3) (Fig. 10C and Table 3). The binding constant is surprisingly variable in the presence of Eosin Y, while a smaller influence in the presence of ibuprofen (somewhat lower than with isolated BSA). The result indicates that the binding site of complex is mainly located within site I of BSA.

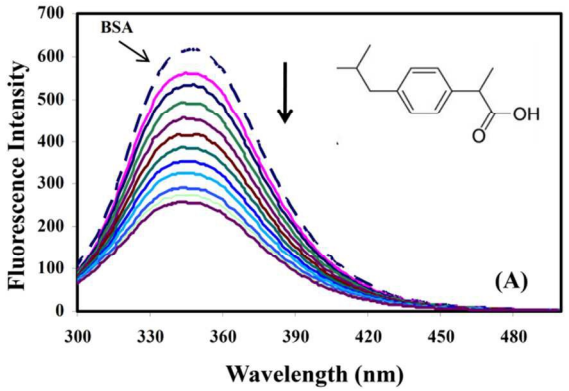

421

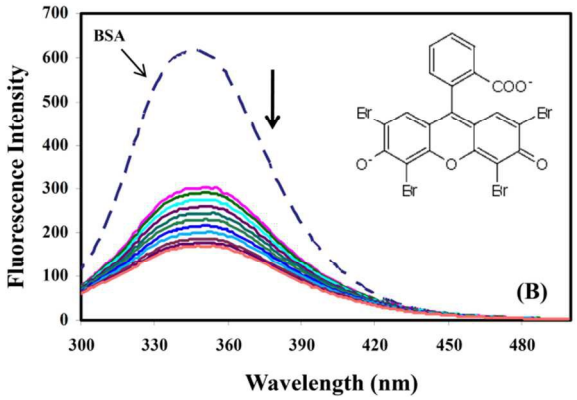

422

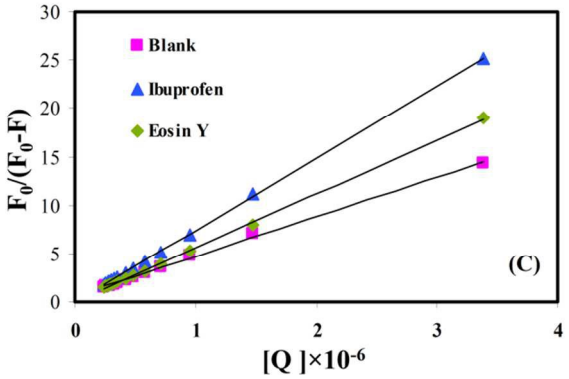

423

424

425 **Fig. 10.** Influence of selected site markers on the fluorescence of compkex boundto BSA
426 (T=298K, λ_{ex} = 285 nm). (A) C(BSA) = C(Eosin Y) = 2×10^{-6} mol L^{-1}; (B)C(BSA) =
427 C(Ibuprofen) = 2×10^{-6} mol L^{-1}; C(comlex) 0,2.95×10^{-7} ,6.76×10^{-7},1.04×10^{-6},1.39×10^{-6},1.73×10^{-6},2.06×10^{-6},2.37×10^{-6},2.83×10^{-6} mol L^{-1}.(C) Modified Stern–Volmer plots for the complex–BSA

system in the absence and presence of site markers (T = 298 K, pH 7.4).The inserts correspond to the molecular structures of site markers.

Table 3. Estimated binding constants for site marker competitive experiments of Pd complex-BSA system

Site marker	K_{sv} (L mol $^{-1}$)	K_a(L mol $^{-1}$)	R^a
Blank	5.16×10^5	1.89×10^5	0.9981
ibuprofen	3.03×10^5	2.37×10^4	0.9998
Eosin Y	2.22×10^5	1.91×10^4	0.9995

$R^a$is the correlation coefficient.

The effect of complex on BSA conformation. The synchronous fluorescence spectra are frequently used to characterize the interaction between fluorescence probe and proteins because it can give information about the molecular microenvironment in the vicinity of the chromophores molecules [93].The synchronous fluorescence spectra offer the characteristics of tyrosine residues and the tryptophan residue of BSA when the wavelength interval (Δλ) is 15 nm and 60nm, respectively ($\Delta\lambda=\lambda_{emission} - \lambda_{excition}$). (Fig. 11A and B) shows the effect of the complex on the fluorescence emission for tyrosine and tryptophan in BSA structure. The fluorescence intensities of both tyrosine and tryptophan decrease and the emission wavelength exhibita slight red shift, which indicates that tyrosine and tryptophan residues are placed in a more hydrophobic environment and their micro-environment is rearranged [94], thus resulting in the conformational changes of BSA, thus resulting in the conformational changes of BSA.

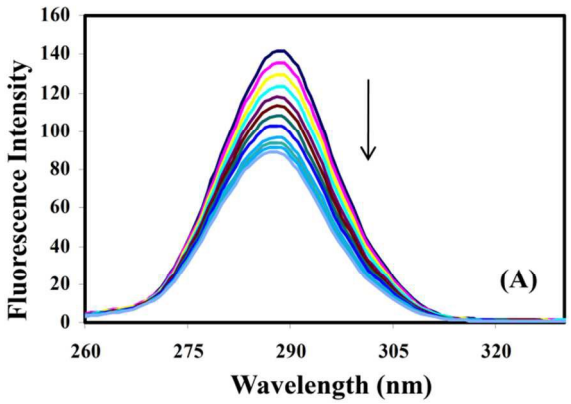

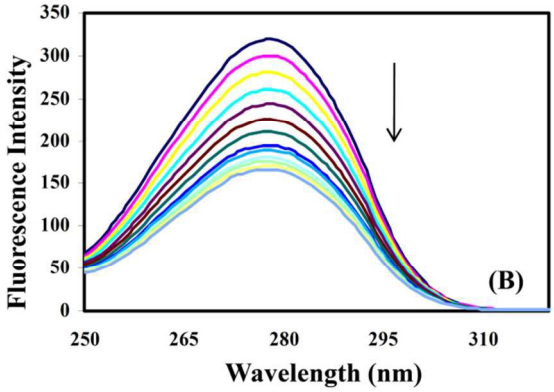

Fig.11. Synchronous fluorescence spectra of BSA in the presence ofdifferent concentrations of complex (λ= 15 nm (A) and λ= 60 nm (B)) at 298 K and pH 7.4. *C*(BSA) = 2×10^{-6} mol L^{-1};*C*(comlex) =0,2.95×10^{-7},6.76×10^{-7},1.04×10^{-6},1.39×10^{-6},1.73×10^{-6},2.06×10^{-6},2.37×10^{-6},$2.83\times10^{-6}$$3.05\times10^{-6}$$3.26\times10^{-6}$$3.47\times10^{-6}$$3.67\times10^{-6}$ mol L^{-1}.

Molecular docking of the Pd (II) complex with DNA sequence d(CGCGAATTCGCG)$_2$. In order to obtain the binding site, the blind docking was performed on the DNA duplex with sequence d(CGCGAATTCGCG)$_2$. The grid map was set to 30×26× 30 $Å^3$ along the x, y, and z axes with 1.0Å grid spacing. The conformations were ranked based on the lowest free binding energy. The results of docking model revealed that the Pd complex fitted into the DNA major

groove (Fig. 12).There are four of hydrophobic interactions between the complex atoms and bases of DNA. (i)between C25, C26 and DG4, (ii) between C9, C10, C11, C35 and DT7, (iii) between C34 and DT8, (iv)between C15, C16and DG16.The binding free energy was found to be-6.98 kcalmol^{-1}, which corresponded to $K_{binding}$=1.30×10^{5} M^{-1}. The binding free energy indicates a high binding affinity between DNA and the Pd complex.

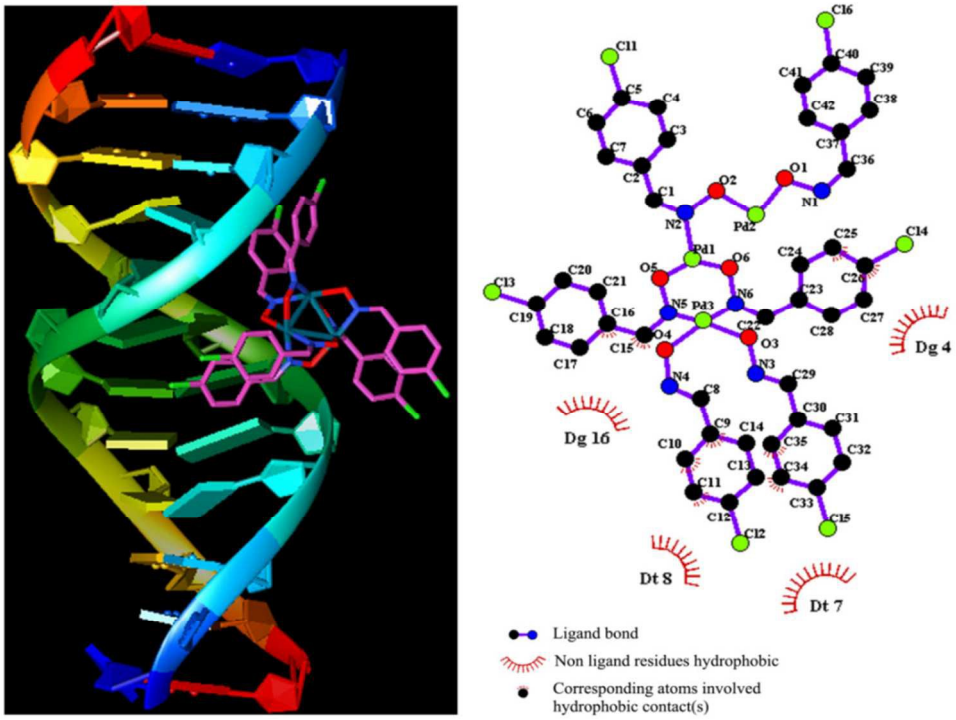

Fig.12.(A) Molecular docking of the Pd complex with the major groove side of DNA by UCSF chimera, (B) two-dimensional interactions generated by LIGPLOT+.

Molecular docking of the Pd (II) complex with BSA. In the docking of Pd (II) complex with BSA, a grid map 52 × 30 × 32 Å^{3}was created with a grid-point spacing of 1.0 Å. The conformations were ranked based on the lowest binding free energy. The molecular docking

study of BSA showed that the Pd (II) complex prefered the binding pocket of domain I. As shown in (Fig. 13), there are seven hydrophobic interactions between the complex atoms and the amino acids of binding site: (i) between C29, C30, C34 and Gln165, (ii) betweenC15, C16, C17, C21 and Gly162, (iii) betweenC15and Ans158, (iv) betweenC41 and Trp134, (v) between C39 andGlu17, (vi) between C38 and Lys131, (vii) between C17, C18 and Lys159.The binding free energy for the complex to BSA was found to be –5.96kcal mol^{-1}. Also, the docking study shows that the distance between the Trp134 residue and the complex is 2.5Å; this finding provides a good agreement with the fluorescence quenching of BSA emission in the presence of the Pd complex.

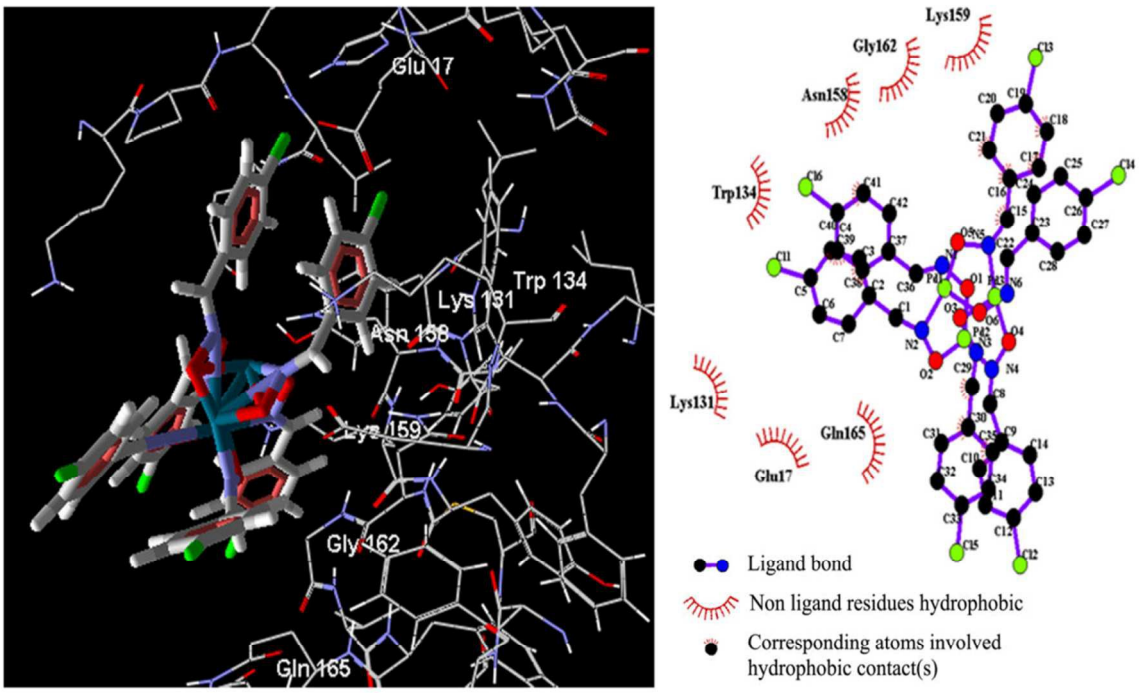

Fig.13. (A) The Pd complex was docked in the binding pocket of BSA using MVD, (B) two-dimensional interactions generated by LIGPLOT+.

Conclusion

Chelate palladium compounds are inorganic agents that have good clinical effects in treatment of various types of cancer as cytotoxic agent, because of chelating ligands to minimize the high lability and fast hydrolysis of palladium complexes in biological environments. In this work, we have synthesized a novel trinuclear palladium (II) complex containing oxime chelate ligand. The structure of the complex was characterized by X-ray crystallography and other methods. The binding interaction of a biologically relevant new Pd complex with calf thymus DNA, bioactivity investigation by UV-Vis and fluorescence spectroscopy, and other spectroscopic measurements unambiguously suggested the groove binding of the probe with the DNA. Molecular docking simulation corroborated the experimental results. The reactivity towards BSA revealed that the quenching of BSA fluorescence by the Pd complex was of the static type. The site marker displacement experiments suggested the location of the complex binding to BSA was the Sudlow ' s site I in the subdomain IIA. Finally, the molecular docking experiment supported the above results and effectively proved the binding of Pd (II) complex to BSA and DNA. New therapeutic approaches are rapidly emerging, and further research may help in designing more specific chelate palladium compounds that would spare the normal tissues, have less adverse effects and improve patient′s quality of life. Further studies on the trinuclear palladium complex in vivo and in vitro anticancer activities are currently in progress in our research group.

Acknowledgments

Funding of our research from the Isfahan University of Technology (IUT) and to the Institute of Biochemistry and BiophysicsUniversity of Tehran are gratefully acknowledged. Crystallography was supported from Czech Science Foundation project No. 14-03276S.

Appendix A. Supplementarymaterial

CCDC 1058050 contains the supplementarycrystallographic data for complex. These data canbeobtained free of charge from the Cambridge Crystallographic Data Center via www.ccdc.cam.ac.uk/data_request/cif.

References

[1] L. O.'Driscoll and M. Clynes, Chemotherapy., 2006, 52, 125-9.

[2] V. F. Chekhun and Yu. V. Shishova, Oncology., 2000, 2, 11-5.

[3] J. Jpn, Cancer Res., 1999, 90 , 1373-1379.

[4] P. J. Loehrer and L. H. Einhorn, Ann. Int. Med., 1984, 100, 704-713.

[5] F. M. Muggia and Semin. Oncol., 1991,18 , 1-4.

[6] R. P. Wernyj and P. J. Morin, Drug Resist. Updat., 2004, 7, 227-232.

[7] W. M. Beck, J. C. Calabrese and N. D. Kottmair, Inorg. Chem., 1979, 18, 176-182.

[8] P. D. Beer, N. C. Fletcher, M. G. B. Drew and T. J. Wear, Polyhedron., 1997, 16, 815-823.

[9] Z. Qin, M. C. Jennings and R. J. Puddephatt, Inorg. Chem., 2001, 40, 6220-6228.

[10] L. Szucova, Z. Travnicek, M. Zatloukal and I. Popa, Bioorg. Med. Chem., 2006, 14, 479-491.

[11] F. Huq, H. Tayyem, P. Beale and J. Q. J Yu, Inorg. Biochem., 2007, 101, 30-35.

[12] M. Sebastian, in nanomedicine and cancer therapy, ed. N. Ninan and E. Elias, Taylor & Francis, edn., 2012, vol. 2, ch. 7, pp. 78-80.

[13] E. Gao, C. Liu, M. Zhu, H. Lin, Q. Wu, L. Liu. Anti - Cancer Agents Med Chem., 2009, 9, 356−368.

[14] A. Garoufis, S. Hadjikakou, N. Hadjiliadis., Coord. Chem. Rev. 2009, 253, 1384−1397.

.

[15] J. Ruiz, N. Cutillas, C. Vicente, M. D. Villa, G. Lopez, J. Lorenzo, F. X. Aviles, V. Moreno, D. Bautista, Inorg. Chem., 2005, 44, 7365−7376.

[16] J. H. Tan, Y. J. Lu, Z. S. Huang, L. Q. Gu and J. Y. Wu, Eur. J. Med. Chem., 2007, 42, 1169-1175.

[17] M. Kurtoğlu and S. A. Baydemir, J. Coord. Chem., 2007, 60, 655-665.

[18] N. M. Krstic, M. S. Bjelakovic, Z. Zizak, M. D. Pavlovic, Z. D. Juranic and V. D. Pavlovic, Steroids., 2007, 72, 406-414.

[19] S. Grigalevicius, S. Chierici, O. Renaudet, R. Lo-Man, E. Deriaud, C. Leclerc and P. Dumy, Bioconjugate. Chem., 2005, 16, 1149-1159.

[20] J. Reedijk, Inorg. Chim. Acta., 1992, 200, 873-881.

[21] P. Vetrovsky, J. L Boucher, C. Schott, P. Beranova, K. Chalupsky, N. Callizot, B. Muller, G. Entlicher, D. Mansuy and J. C. Stoclet, J. Pharm. Exp. Ther., 2002, 303, 823-830.

[22] T. W. Hambley, E. C. H Ling, S. O'Mara, M. J. McKeage and P. J. Russell, J. Biol. Inorg. Chem., 2000, 5, 675-681.

[23] N. Saglam, A. Colak, K. Serbest, S. Duelger, S. Guener, S. Karaboecek and A. O. Belduez, BioMetals., 2002, 15, 357-365.

[24] P. A. Ochoa, S. S. Alexandre, C. Pastor and F. Zamora, J. Inorg. Biochem., 2005, 99 , 2226–2230.

[25] G. B. Onoa, V. Moreno, E. Freisinger and B. Lippert, J. Inorg. Biochem., 2002, 89, 237–247.

[26] X. L. Wei, J. B. Xiao, Y. F. Wang and Y. L. Bai, SpectrochimActa Part A:Mol. Biomol. Spectrosc., 2010, 75, 299–304.

[27] P. B. Kandagal, S. Ashoka, J. Seetharamappa, S. M. T. Shaikh, Y. Jadegoud and O .B.Ijare, J. Pharma. Biomed., 2006, 41, 393-399.

[28] X. J. Guo, A. J. Hao, X. W. Han, P. L. Kang, Y. C. Jiang and X. J. Zhang, Mol. Biol. Rep., 2011, 38, 4185-4192.

[29] K. Karami, M. Hosseini-kharat, H. Sadeghi-Aliabadi, J. Lipkowski and M. Mirian, Polyhedron., 2012, 50, 187-192.

[30] K. Karami, M. Hosseini-kharat, H. Sadeghi-Aliabadi, J. Lipkowski and M. Mirian, Eur. J. Med. Chem., 2014, 73, 8-17.

[31] F. Shahsavar, M. Bozorgmehr, E. Mirzadegan,A. Abedi, Z. Mehri Lighvan, F. Mohammadi, N.Safari,V.Amani, A.H. Zarnani., Anti - Cancer Agents Med Chem. DOI: 10.2174/1871520615666150807104228 ·

[32] M. M. Hania, E- J. Chem., 2009, 6, 508-514.

[33] S. Satyanarayana, J. C. Dabroniak and J. B. Chaires, Biochemistry., 1992, 31, 9319-9324.

[34] L. Palatinus and G. Chapuis, J. Appl. Cryst., 2007,40, 786-790.

[35] V. Petricek, M. Dusek and L. Palatinus, Z. Kristallogr. 2014, 229, 345-352.

[36] J. Rohlicek and M. Husak, J. Appl. Cryst., 2007, 40, 600-601.

[37] G. M. Morris, D. S. Goodsell, R.S. Halliday, R. Huey, W.E. Hart, R.K. Belew and A.J. Olson, J. Comput. Chem., 1998, 19, 1639-1662.

[38] http://www.molegro.com/index.php of Computational Chemistry 2004, 25, 1605-1612.

[39] E.F. Petterson, T. D. Goddard, C. C. Huang and G.S. Couch, J. Comput. Chem., 2004, 25, 1605-1612.

[40] R. A. Laskowski and M. B. Swindells, J. Chem. Inf. Model. 2011, 51, 2778-2786.

[41] D.V. Spoel, E. Lindahl, B. Hess, G. Groenhof, A.E. Mark and H.J.C. Berendsen, J. Comput. Chem., 2005, 26, 1701–1718.

[42] V. Hornak, R. Abel, A. Okur, B. Strockbine, A. Roitberg and C. Simmerling, Proteins: Struct. Funct. Bioinform. 2006, 65, 712–725.

[43] T. Darden, D. York and L. Pedersen, J. Chem. Phys., 1993, 98, 10089–10092.

[44] U. Essmann, L. Perera, M. L. Berkowitz, T. Darden, H. Lee and L.G. Pedersen, J. Chem. Phys., 1995, 103, 8577–8593.

[45] W. C. Swope, H. C. Andersen, P. H. Berens and K. R. Wilson, J. Chem. Phys., 1982, 76, 637–649.

[46] E. H. Kennard, Kinetic theory of gases, McGraw-Hill, New York, 1963.

[47] K. Huang, Statistical mechanics, Wiley, New York, 1963.

[48] L. Rivail, C. Chipot, B. Maigret, I. Bestel, S. Sicsic and M. Tarek, J. Mol. Struct. (Theochem)., 2007, 817, 19–26.

[49] H.J.C. Berendsen, J.P.M. Postma, W.F.V. Gunsteren, A.D. Nola and J.R. Haak, J. Chem. Phys., 1984, 81, 3684-3690.

[50] H. Onoue, K. Mmamiand and K. Nakagawa, Bull Chem Soc Japan., 1970, 43, 3480-3485.

[51] A. G. Constablew, W. G. Mcdonaldl, L. C.. Sawkins and B. L Shaw. J.C.S. Chem. Comm., 1978, 1061-1062.

[52] H. Chao, W. J. Mei, Q. W. Huang and L. N. Ji, J. Inorg. Biochem., 2002, 92, 165-170.

[53] P. Drevensek, N. Poklar Ulrih, A. Majerle and I. Turel, J. Inorg. Biochem., 2006, 100, 1705-1713.

[54] I. D. Vilfan, P. Drevensek, I. Turel and N. Poklar Ulrih, Biochim. Biophys. Acta, GeneStruct. Expr. 2003, 1628, 111-122.

[55] Y. Song, Q. Wu, P. Yang, N. Luan, L. Wang and Y. Liu, J. Inorg. Biochem., 2006, 100 ,1685-1691.

[56] T. M. Kelly, A. B. Tossi, D. J. McConnell and T. C. Strekas, Nuc. Acids Res., 1985, 13, 6017- 6034.

[57] S. S. Mati, S. S. Roy, S. Chall, S. Bhattacharya and S. C. Bhattacharya, J. Phys. Chem. B, 2013, 117, 14655-14665.

[58] S. Bhattacharya, G. Mandal and T. Ganguly, J. Photochem. Photobiol.B: Biol., 2010, 101 , 89-96.

[59] S. Ghosh, P. Kundu, B. Kumar Paul and N. Chattopadhyay, RSC Adv. 2014, 4, 63549-63558.

[60] A. Wolfe, G. H. Shimer and T. Meehan, Biochemistry., 1987, 26, 6392–6396.

[61] R. Rohs and H. Sklenar, J. Biomol. Struct. Dyn., 2004, 21, 699-711.

[62] E. Long and J. Barton, Acc. Chem. Res., 1990, 23, 271-273.

[63] Z. M. Lighvan, A. Abedi and M. Bordbar, Polyhedron., 2012, 42, 153-160.

[64] E. C. Long and J. K. Barton, Acc. Chem. Res., 1990, 23, 271–273.

[65] A. M. Polyanichko, V. V. Andrushchenko, E. V. Chikhirzhina, V. Vorobev and H. Wieser, Nuc. Acids Res., 2004, 32, 989-996.

[66] K. Karidi, A. Garoufis, A. Tsipis, N. Hadjiliadis, H. Dulk and J. Reedijik, Dalton Trans., 2005, 7, 1176-1187.

[67] A.D. Richards and A. Rodger, Chem. Soc. Rev., 2007, 36, 471–483.

[68] P.U. Maheswari and M. Palaniandavar, J. Inorg. Biochem., 2004, 98, 219–230.

[69] Z. Zhang and X.H. Qian, Int. J. Biol. Macromol., 2006, 38, 59–64.

[70] A.L. Lehninger, D.L. Nelson, M.M. Cox, Principles of Biochemistry, New York,1993.

[71] M.V. Volkenshtein, Biophysics , Moscow: Mir, 1983.

[72] C.V. Kumar and E.H. Asuncion, J. Am. Chem. Soc., 1993, 115, 8547-8553.

[73] P. Kumar, I. Gorai., M.K. Santra, B. Mondal and D. Manna., Dalton Trans., 2012, 41, 7573-7581.

[74] J. L García-Giménez, G. Alzuet, M. Gonzáles-Alvarez, M. Liu-Gonzáles, A.Castiñeiras and J. Borrás, J. Inorg. Biochem., 2009, 103, 243-255.

[75] A. Bodoki, A. Hangan, L. Oprean, G. Alzuet, A. Castiñeiras and J. Borrás, Polyhedron., 2009, 28, 2537-2544.

[76] W. Zhang, F. Wang, X. Xiong, Y. Ge and Y. Liu. J. Chil. Chem. Soc., 2013, 2, 1717-1721.

[77] F. Samari, B. Hemmateenejad, M. Shamsipur, M. Rashidi and H. Samouei., Inorg Chem. 2012, 51, 3454-3464.

[78] Y. He, Y. Wang, L. Tang, H. Liu, W. Chen, Z. Zheng and G. Zou. J Fluoresc., 2008, 18, 433-442.

[79] Y.Y. Yue, X.G. Chen, J. Qin and X.J. Yao .D**yes** Pigm., 2008,79, 176-182.

[80] X.W Li, X.J Li, Y.T Li, Z.Y Wu and C.W Yan. J. Photochem.Photobiol B., 2013, 118, 22–32

[81] J. Toneatto and G.A. Arguello, J. Inorg. Biochem., 2011, 105, 645–651.

[82] T. Peters, Adv. Protein Chem.,1985, 37,161-245.

[83] S. S. Bhat, A.A. Kumbhar, H. Heptullah, A.A. Khan, V.V. Gobre, S.P. Gejji and V.G. Puranik, Inorg. Chem., 2011, 50, 545–558.

[84] J. R. Lakowicz and G.Weber, Biochemistry., 1973, 12, 4161–4170.

[85] J. R. Lakowica, Principles of Fluorescence Spectroscopy, 2nd ed., Plenum Press, New York, 1999, pp. 237–265.

[86] S. Deepa and A.K. Mishra, J. Pharm. Biomed. Anal., 2005, 38, 556–563.

[87] S. Lehrer, Biochemistry., 1971, 10, 3254–3263.

[88] A. Belatik, S.Hotchandani, J. Bariyanga, and H.A. Tajmir-Riahi, Eur. J. Med. Chem., 2012, 48, 114–123.

[89] F. F. Tian, F. L. Jiang, X. L. Han, C. Xiang, Y. S. Ge, J. H. Li, Y. Zhang, R. Li, X.L. Ding and Y. Liu, J. Phys. Chem., B. 2010, 114, 14842–14853.

[90] G. Sudlow, D. J. Birkett and D. N. Wade, Mol. Pharmacol., 1976, 12, 1052–1061.

[91] X. M. He and D. C. Carter, Nature., 1992, 358, 209–215.

[92] G.W. Zhang and Y.D. Ma, Food Chem., 2013, 136, 442–449.

[93] N. Wang, L. Ye, B. Q. Zhao, J.X. Yu, Braz. J. Med. Biol. Res., 2008, 41, 589-

[94] J. Q. Liu, J. N. Tian, Z. D. Hu, and X. G. Chen, Bioorgan. Med. Chem., 2004, 73, 443-450.

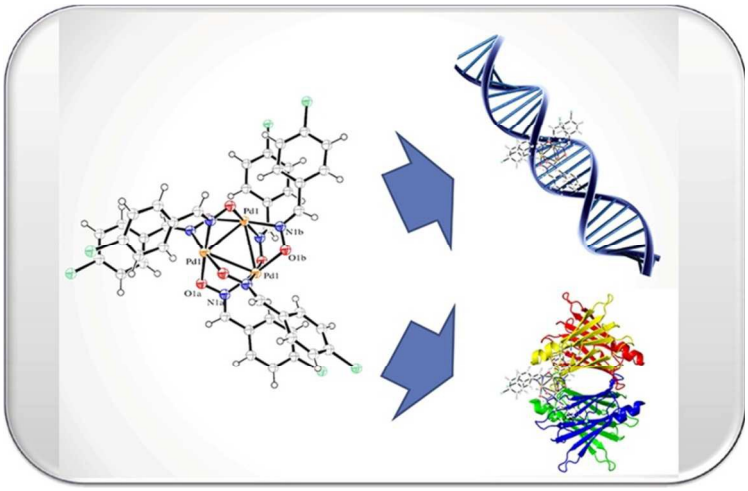

The trinuclear palladium (II) complex containing oxime ligand, showed significant interaction with both CT-DNA and BSA. The molecular docking indicates high binding affinity between DNA and BSA with Pd complex.